Pergamon

0301-9322(93)E0015-W

Int. J. Multiphase Flow Vol. 20, No. 3, pp. 593–612, 1994

0301-9322/94 $7.00 + 0.00

A COUPLED TWO-PHASE SHEAR LAYER/LIQUID FILM CALCULATION METHOD. FORMULATION OF THE PHYSICAL PROBLEM AND SOLUTION ALGORITHM

CH. MALAMATENIOS, K. C. GIANNAKOGLOU and K. D. PAPAILIOU
Laboratory of Thermal Turbomachines, National Technical University of Athens, P.O. Box 64069, 15710 Athens, Greece

(Received 1 November 1992; in revised form 11 November 1993)

Abstract—A coupled two-phase shear layer/liquid film calculation method is presented for the prediction of the simultaneous motion of a wavy liquid film and the two-phase stream flowing above it. Conservation equations, for both the shear layer and the liquid film, are cast in a compatible integral form and solved together through a space-marching technique. The system of equations resulting for both streams is enhanced through a set of semi-empirical models, appropriately modified to match the proposed method, in order to effect closure. These models deal with various physical aspects including (a) velocity profiles within the liquid film, (b) the structure of the interface and (c) any exchange of information between the two streams. Evaluation of the method is performed in cases where liquid films are developed along flat surfaces, for which measurements and/or numerical results are available.

Key Words: two-phase flow, shear layer, liquid film, interfacial waves, roughness, deposition

1. INTRODUCTION

Motion of fluids in the form of a liquid film, developing along solid walls of various shapes and orientations, is often encountered in quite a few processes and engineering systems. Applications may be found in thermal desalination and drying systems, nuclear reactors and in gas absorption and desorption related problems. Liquid film flows have a significant influence on heat and mass transfer processes and contribute to erosion and corrosion problems. In the turbomachinery field, the dry steam which expands below the saturation line, within the low-pressure stages of a steam turbine, results in the formation of water droplets which, in turn, form liquid films along the blades and the casing walls (Moore & Sieverding 1976). These films are developing under the influence of the high-velocity wet-steam flow; in their motion they collect droplets, either new ones from the flowing steam or those entrained from the previous stages. At very high gas velocities, atomization of the film occurs that forces lumps of water to re-enter into the core flow.

During the last few decades, considerable experimental and/or numerical work has been carried out in this field and research was oriented mainly towards annular (Chu & Dukler 1975; Henstock & Hanratty 1976) or stratified (Andritsos & Hanratty 1987a; Cheremisinoff & Davis 1979) film flows in pipes at various inclinations. These studies intended to improve nuclear reactor safety. The free-falling or shear-driven film behaviour along inclined or horizontal plates was also the subject of numerous works (Khoshaim & Ryley 1976; Wittig *et al.* 1991), since it is involved in several chemical and mechanical engineering applications.

The calculation of a liquid film, driven by the shear stress of a concurrently flowing two-phase stream, requires the strongly coupled solution of the two adjacent flow regimes. Most of the published works in this domain deal with the liquid film modelling and often overcome the shear layer solution using appropriate empirical information (Ryley & Patel 1971; Hammitt *et al.* 1975). They are merely based on integral approaches, expressing the film volume flow rate conservation (in the case of no mass exchange) or evolution (in the case of mass exchange). From a numerical point of view, these formulations are oversimplified and the implemented physical models and assumptions dictate the difference between them. The necessary empiricism covers various physical aspects, starting from simple ones (like the velocity profile used for the liquid film) up to more

complex ones (like the identification of the type of interfacial waves and the study of film atomization). Models are constantly being proposed (Dobran 1983; Andreussi *et al.* 1985; Brauner *et al.* 1985; Jurman & McCready 1989) for the examination of the above specific topics. On the other hand, there are methods which handle the gaseous stream with sophisticated numerical tools, like (parabolized) Navier–Stokes solvers with appropriate turbulence modelling (Witting *et al.* 1991). These methods minimize the involved empiricism and constitute accurate procedures for the prediction of the coupled evolution of the two streams. The strong coupling between them requires successive solutions of the Navier–Stokes equations, leading to time-consuming calculations. In addition, in most of the above-mentioned works, the stream driving the film is a single-phase one, namely air or dry steam.

The purpose of the present paper is to introduce a fully coupled shear layer/liquid film integral calculation method. The film is developing along a solid surface under the influence of a concurrent single- or two-phase stream and any mass or/and momentum transfer along their interface is appropriately modelled. Emphasis is put on the liquid film analysis rather than the shear layer one and the coupling procedure. The method is based on the "three-zone" approach, where the flow system is considered as decomposed in three adjacent parts, namely the inviscid zone, the shear layer and the liquid film. Each zone is described by its own physical model and particular attention is paid to the way information travels between adjacent zones. Horizontal or inclined plane, stratified flows may be handled by the present method. The analysis aims to represent complex flows, such as those encountered in steam turbines, while avoiding the time-consuming solution of Navier–Stokes equations. The liquid film is either supplied at a certain location or/and formed by droplets coming into contact with the solid walls. Validation of the method, either as a whole or in terms of the various implemented submodels, is finally presented.

2. THE THREE-ZONE MODEL

The decomposition of the flow domain into an inviscid and a viscous part was first introduced by Prandtl (1904) for single-phase flows. Since then, it has been widely used in engineering applications, due to the fact that it requires less computing time than the solution of the full Navier–Stokes equations. In the absence of a liquid film, the two-zone approach was previously extended by the authors to cover two-phase flows (Malamatenios *et al.* 1990, 1992). In these works, the possibility of using semi-empirical information, already developed for single-phase flows, in the case of two-phase flows as well, was discussed and justified.

The liquid film comes to add its own contribution to the complexity of the flow domain by creating a third zone which interferes between the shear layer and the solid wall. It manifests its presence by producing a new boundary for the shear layer which is rough, the degree of roughness depending on the waviness of the film surface. Furthermore, this boundary is moving and the shear layer has to be considered as developing along a moving rough wall. Figure 1 presents the three-zone concept in a simplified but descriptive manner. Various additional flow features, like droplets leaving the liquid film and entrained into the core flow or droplets deposited onto the film also appear, in order to give a generalized picture of the physical phenomena that might occur.

It is worth listing the basic assumptions governing the three-zone structure:

(a) The external flow zone (zone I) is not directly influenced by the presence of the liquid film (zone III). The liquid film directly influences only the shear layer (zone II).
(b) If a two-phase/liquid film flow is studied, droplets are treated in a Langrangian way in both the external flow (zone I) and the shear layer (zone II). Droplets impinging on the interface do join the liquid film. Nevertheless, during the external flow solution, they are handled through appropriate numerical boundary conditions.
(c) The transpiration velocity technique (Lock & Williams 1987) is used for the coupling of zones I and II, as if the liquid film were absent.
(d) From the shear layer point of view, the liquid film is seen as a rough boundary, moving with the interfacial velocity, which varies with streamwise distance. The

shear layer, in turn, manifests its influence on the liquid film by providing the driving force.

A continuous exchange of information is thus necessary in order to model two-phase/liquid film flows. The two-phase inviscid solution (zone I) provides the viscous flow calculation with the gaseous phase velocity and pressure distribution at the edge of the shear layer, as well as with the droplet size, temperature, velocity vector and number density distribution along the whole length of the solid boundary. At each computational location, the shear layer (zone II) provides the liquid film (zone III) with the interfacial stress, the streamwise pressure gradient and the increase in liquid flux caused by the deposition of droplets. The liquid film provides the shear layer with the roughness (necessary for the momentum coupling between the film and the shear layer), the interfacial velocity and the film thickness. Besides, if film atomization occurs, the liquid film calculation must also provide information about liquid mass entrained in the gaseous stream; the atomization process is not studied at present.

The integral formulation of the viscous part of the flow constitutes a parabolic problem in space, for both the two-phase shear layer and the liquid film. The computational procedure requires the solution of two integral equations for the gaseous phase, in conjunction with the transport equations for the droplets, while for the liquid film two additional integral equations are formulated and solved simultaneously with the shear layer's ones. Thus, a space-marching technique is established, for the prediction of the motion of shear-driven liquid films in turbulent, dispersed two-phase flows. The procedure to be described here deals with two-phase streams, but when the droplets' transport equations are omitted, the same algorithm can also handle liquid films driven by single-phase flows.

3. THE TWO-PHASE SHEAR LAYER ANALYSIS

3.1. Governing equations

The gaseous phase conservation equations are first written in a curvilinear coordinate system (s, n), the s-lines of which coincide with the real flow streamlines. The subtraction of these equations, as written for the external-inviscid and the real-viscous flow, results in the corresponding deficit equations which are integrated along the normal to the streamwise direction (n). No further details are given here, since this part of the method is analysed in previous publications, as

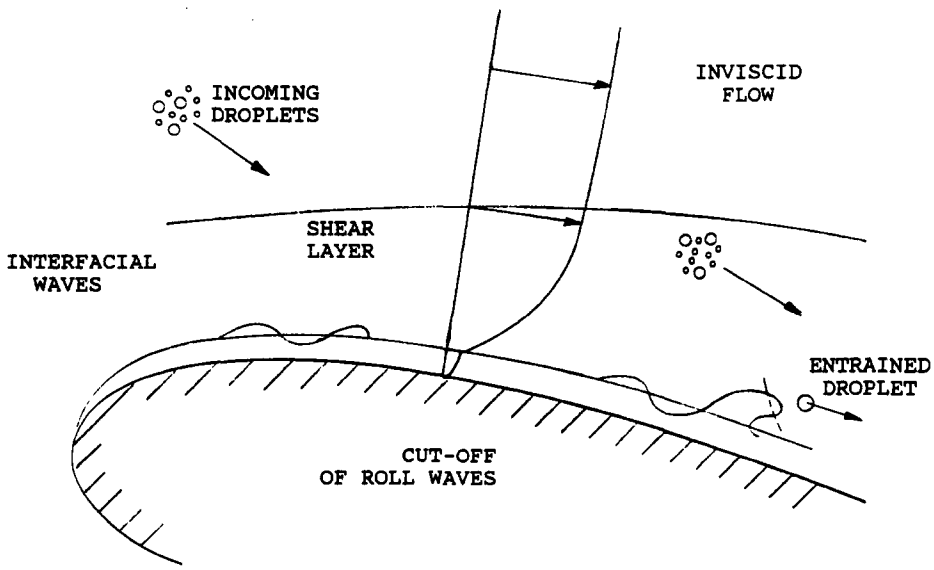

Figure 1. The three-zone concept for the liquid film calculation method.

mentioned above; nevertheless, for the sake of completeness, the resulting integral equations are listed below:

(a) the streamwise momentum integral equation,

$$\frac{\mathrm{d}(\epsilon_e \rho_e V_{S_e}^3 \delta_2)}{\epsilon_e \rho_e V_{S_e}^3 \delta_2} + (H_{12} - 1)\frac{\mathrm{d}V_{S_e}}{V_{S_e}} = \frac{C_f}{2\delta_2}\mathrm{d}s + A_M + G_M \quad [1]$$

and

(b) the mean-flow kinetic energy integral equation,

$$\frac{\mathrm{d}(\epsilon_e \rho_e V_{S_e}^3 \delta_3)}{\epsilon_e \rho_e V_{S_e}^3 \delta_3} + r(\gamma - 1)M_e^2 \frac{\mathrm{d}V_{S_e}}{V_{S_e}} = \frac{C_D}{\delta_3}\mathrm{d}s + A_E + G_E, \quad [2]$$

where V_S, ρ and ϵ stand for the streamwise velocity, gas density and void fraction, while γ and r denote the ratio of the specific heats of the gases and a recovery factor (Papailiou & Bouras 1990), respectively. As to source terms, G_M and G_E express the effect of the dispersed phase on the continuous one, while A_M and A_E group together the influences of surface curvature and the normal fluctuation terms on the gaseous phase shear layer. The subscript e denotes values corresponding to the external (inviscid) flow.

The definitions of the displacement, momentum and energy thicknesses ($\delta_1 = H_{12}\delta_2$, δ_2 and δ_3, respectively) and of the other integral quantities (friction coefficient C_f and dissipation factor C_D), remain unchanged from the description for the two-phase flow case by Malamatenios *et al.* (1992). Nevertheless, it has to be pointed out that, when the two-phase shear layer is developing above a liquid film, integrations along the normal (n) direction are based on a gaseous phase velocity profile properly modified to account for the waviness of the shear layer/liquid film interface and the moving frame of reference. This will become clearer after perusal of section 3.2.

3.2. Modifications due to the presence of the film

(a) By analogy to the way wall roughness is modelled in single-phase turbulent flows, a modification is employed to the shear layer velocity profile in order to account for the roughness of the interface. In particular, a modified version of the Coles' (1955, 1956) velocity profile is used, with the generalized form

$$u^+ = f(n^+, \delta^+) - \Delta u^+, \quad [3]$$

where Δu^+ denotes the shift of the logarithmic profile, caused by the introduction of roughness in the law of the wall, according to Schlichting (1979). For the fully rough case, the change in the intercept Δu^+ takes the form

$$\Delta u^+ = \frac{1}{\kappa}\ln\frac{k_S u_\tau}{\nu_i} + D, \kappa = 0.41, \quad D = -3, \quad [4]$$

as a function of an equivalent sand-grain roughness k_S. The latter is provided from the liquid film calculation, once the film wavy surface structure is known, by means of an appropriate model. The calculation of k_S entails a complete knowledge of the liquid film characteristics and is deferred to a later section.

(b) For shear layer flows in the absence of a liquid film, the non-dimensional quantities are all defined relative to the wall conditions. When the shear layer is developing above a moving film, the quantities must be defined relative to the interface conditions. Thus, the gaseous phase velocity profile becomes

$$u^+ = \frac{(u - u_i)}{u_\tau}, u_\tau = \left(\frac{\tau_i}{\rho_i}\right)^{1/2}, \quad [5]$$

where u_i is the interface velocity, τ_i is the interfacial stress and ρ_i stands for the gas density. The non-dimensional distance from the film/shear layer interface is defined by

$$n^+ = \frac{(n - \bar{h})u_\tau}{\nu_i}, \quad [6]$$

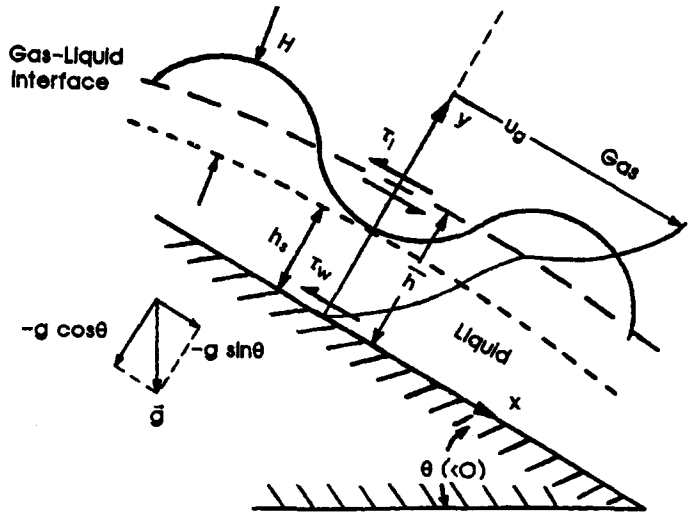

Figure 2. A liquid film in an inclined plane.

with ν_i the gaseous phase kinematic viscosity at the interface and $\bar{h}$ the time-mean film height, to be introduced below.

3.3. *Method formulation*

Using u_τ/V_{S_e} and Re_δ, a Reynolds number based on the shear layer thickness δ, as unknown variables (Bouras 1993), the system of equations [1] and [2] is solved using a Newton–Raphson method. Between two successive computational positions along the solid wall, this system is handled simultaneously with a second one, which governs the liquid film flow (to be analysed in the following section), by introducing a sort of local iteration. The adoption of a two-parameter velocity profile for the gaseous phase, allows the above two quantities to be sufficient in order to establish all the other shear layer properties at a certain location (Papailiou & Bouras 1990).

When the shear layer (zone II) is a two-phase one, droplet equations must be included in the local iterative scheme as well. Droplets are tracked within the shear layer and their trajectories, temperature and diameter evolution are calculated by solving the corresponding transport equations (Crowe 1982). Here, it is assumed that the droplets are sufficiently dispersed and droplet–droplet interaction is negligible; only deposition of droplets reaching the liquid film surface is allowed. The source terms G_M and G_E in [1] and [2] and the void fraction ϵ are obtained as in Malamatenios *et al.* (1992).

4. THE LIQUID FILM ANALYSIS

4.1. *Governing equations and problem formulation*

A rather simple physical flow configuration, where a liquid film is flowing along an inclined plane under the influence of an external interfacial stress, is illustrated in figure 2. This simple problem was considered for the derivation of the governing equations, even if it does not cover all possible liquid film flows. Additional physical aspects (like the curvature of solid walls) have been implemented in the programmed equations, but they are omitted here, for the sake of simplicity.

The film behaviour is dominated by the irregular motion of its interface and is intrinsically time-dependent. Since the exact solution of the unsteady governing equations has to be avoided in industrial computations, the time-mean film thickness $\bar{h}$ is introduced instead and the unsteadiness of the interface is "steadily" modelled through its equivalent sand roughness. In the following, the bars denoting time-mean quantities are omitted, except for cases where emphasis has to be given. Assuming an orthogonal coordinate system (x, y), where x stands for the direction

parallel to the solid surface, the streamwise momentum equation in a steady form for the time-mean quantities reads

$$u\frac{\partial u}{\partial x}+v\frac{\partial u}{\partial y}=-\frac{1}{\rho_L}\frac{\partial P}{\partial x}+\frac{1}{\rho_L}\frac{\partial \tau}{\partial y}-g\sin\theta, \qquad [7a]$$

where the subscript L indicates the liquid phase.

Under the assumption of a sufficiently small slope of the time-mean interface and that of a shallow liquid, the time-mean pressure P at a distance (y) from the solid wall inside the liquid film is given by

$$P=P_i+\rho_L g(\bar{h}-y)\cos\theta, \qquad [7b]$$

where P_i is the pressure at the interface. Equation [7b] results from the integration of the normal momentum equation along the normal to the wall direction. By combining [7a] and [7b], the integral form of the streamwise momentum equation reads

$$\frac{\partial}{\partial x}\int_0^{\bar{h}}u^2\,dy-u_i\frac{\partial}{\partial x}\int_0^{\bar{h}}u\,dy=-\frac{\bar{h}}{\rho_L}\left[\frac{\partial P_i}{\partial x}+\rho_L g\cos\theta\frac{\partial \bar{h}}{\partial x}\right]+\frac{1}{\rho_L}(\tau_i-\tau_w)\ -g\bar{h}\sin\theta, \qquad [8]$$

where τ_w is the mean wall stress.

The integral form of the continuity equation is written as

$$\frac{\partial}{\partial x}\int_0^{\bar{h}}u\,dy-\Delta Q=0; \qquad [9a]$$

ΔQ is the mass exchange between the liquid film and the outer flow and is positive when mass is added to the liquid film. The volumetric flow rate Q per unit width (in m^2/s), is given by

$$Q=\int_0^{\bar{h}}u\,dy. \qquad [9b]$$

It is a matter of rearrangement of [8] and [9a,b], to get the integro-differential equation

$$(\Gamma\bar{u}_\alpha^2-\bar{h}g\cos\theta)\frac{d\bar{h}}{dx}=\frac{1}{\rho_L}\left[(\tau_w-\tau_i)+\bar{h}\frac{dP_i}{dx}\right]+\bar{h}\left(g\sin\theta+\bar{u}_\alpha^2\frac{d\Gamma}{dx}\right)+(2\Gamma\bar{u}_\alpha-u_i)\Delta Q, \qquad [10]$$

which, along with [9a], is solved in order to provide the film time-mean thickness $\bar{h}$ and the wall stress τ_w. The average film velocity $\bar{u}_\alpha$,

$$\bar{u}_\alpha=\frac{1}{\bar{h}}\int_0^{\bar{h}}u\,dy, \qquad [11]$$

and the shape factor Γ, defined by Hanratty (1983) as

$$\Gamma=\frac{1}{\bar{h}\bar{u}_\alpha^2}\int_0^{\bar{h}}u^2\,dy, \qquad [12]$$

appear in the above integral equation. The second variable characterizes the film velocity, taking a value equal to 1.333 for a laminar liquid film. Equation [10] has a strongly non-linear character and is similar to the one proposed by Miya *et al.* (1971) for the instantaneous film thickness. In the latter work, this equation aimed at calculating the geometry of roll waves using empirical information for the driven shear stress.

Equations [9a] and [10] constitute the system of two integral equations which is solved to yield the liquid film properties at each location, once these properties are known at the previous one. This system is solved in terms of the mean thickness $\bar{h}$ and the wall stress τ_w using a Newton–Raphson method, in the context of the local iteration scheme between two successive locations, as introduced in section 3.3. All the remaining quantities are modelled through suitable closure conditions, while the inlet film thickness and flow rate must be specified. For numerical reasons, an infinitesimally small thickness and flow rate need to be provided at the inlet, even if the film is formed solely through deposition of droplets.

It is worth noting that the interface stress τ_i constitutes a direct outcome of the two-phase shear layer solution and an input for the liquid film, at the same time. The pressure gradient (dP_i/dx),

being known from the solution of the external zone I, is also an input for the liquid film calculation. The liquid film calculation provides the two-phase shear layer with the film thickness $\bar{h}$ and the velocity u_i of the film at this height, which are needed for the construction of the shear layer velocity profile from the interface up to the shear layer edge. The interfacial roughness, which models the effect of the waviness of the interface on the turbulence of the shear layer, is also an outcome of the liquid film calculation procedure.

4.2. Liquid film velocity profiles

The calculation of the average film velocity $\bar{u}_\alpha$ and the shape factor Γ requires the assignment of a velocity profile to the liquid film. The adopted profile is based on the decomposition of the film into a continuous and a wavy layer region (Dobran 1983). The single-phase turbulence structure is assumed to be valid in the continuous layer and appropriate modifications to the structure of turbulence are introduced in the wavy layer. More specifically, for the continuous layer of the film the classical expressions of turbulent velocity profile are used:

$$\begin{aligned} u^+ &= y^+, && \text{for} \quad y^+ \leqslant 5 \\ u^+ &= -3.05 + 5.0 \ln y^+, && \text{for} \quad 5 < y^+ \leqslant 30 \\ u^+ &= 5.5 + 2.5 \ln y^+, && \text{for} \quad 30 < y^+ < h_S^+ \end{aligned} \qquad [13]$$

if $h_S^+ > 30$. The non-dimensional distance y^+ is defined by

$$y^+ = \frac{yu^*}{\nu_L}, \quad u^* = \left(\frac{\tau_w}{\rho_L}\right)^{1/2}, \qquad [14]$$

with u^+ the dimensionless film velocity ($u^+ = u/u^*$) and ν_L the kinematic viscosity of the liquid phase.

In the wavy layer region, the eddy viscosity is supposed to be proportional to the thickness of this layer. Thus, the following expression for the velocity inside the wavy layer is obtained:

$$u^+ = u^+(h_S^+) + \frac{(y^+ - h_S^+)}{\left(\dfrac{\mu_{eff}}{\mu_L}\right)_{wL}} \cdot \left[1 - \left(1 - \frac{\tau_i}{\tau_w}\right)\frac{y^+ + h_S^+}{2\bar{h}^+}\right], \qquad [15]$$

where $(\mu_{eff}/\mu_L)_{wL}$ is the effective diffusivity for the wave layer and $\bar{h}^+$ is the dimensionless film thickness. The $(\mu_{eff}/\mu_L)_{wL}$ ratio is related to the $(\bar{h}^+ - h_S^+)$ quantity via the empirical formula

$$\left(\frac{\mu_{eff}}{\mu_L}\right)_{wL} = 1 + C_1(\bar{h}^+ - h_S^+)^n, \qquad [16]$$

where C_1 and n are appropriate constants (Dobran 1983). The substrate film thickness h_S results from the submodels used to describe the wavy shape of the shear layer/liquid film interface.

4.3. Modelling the wavy interface

For sufficiently low gas velocities, no waves are observed at the film surface. As the outer flow velocity increases, two-dimensional, periodic, finite-amplitude waves are observed to cover the film surface. These waves become progressively three-dimensional, at higher stream velocity (Dukler 1972). Finally, a transition occurs from periodic to "roll" or "solitary" waves, which have a highly roughened interface, are not periodic and carry significant fluid with them (Jurman & McCready 1989). At very high stream velocities atomization of the film occurs, which is directly related to the presence of roll waves on the film surface (Woodmansee & Hanratty 1969). According to Andritsos & Hanratty (1987b), a good-for-design-purposes approximation for the gas velocity,

required to initiate irregular large-amplitude waves, is predicted from the inviscid Kelvin–Helmholtz instability. Thus, transition takes place when the gas velocity becomes

$$(U_G - \tilde{u}_a)^2 \leqslant [k^2\sigma + (\rho_L - \rho_G)g]\frac{\bar{H}}{\rho_G}\left[\frac{\tanh(k\bar{H})}{k\bar{H}} + \frac{\rho_G}{\rho_L}\frac{\tanh(k\bar{h})}{k\bar{H}}\right], \quad [17]$$

where U_G and ρ_G are the mean velocity and density of the gas stream, k is the wavenumber, σ is the surface tension of the liquid and $\bar{H}$ is the mean height of the driving stream.

The film velocity profile and the equivalent sand roughness of the interface require a detailed description of the periodic and solitary waves structure. These are briefly presented in appendices

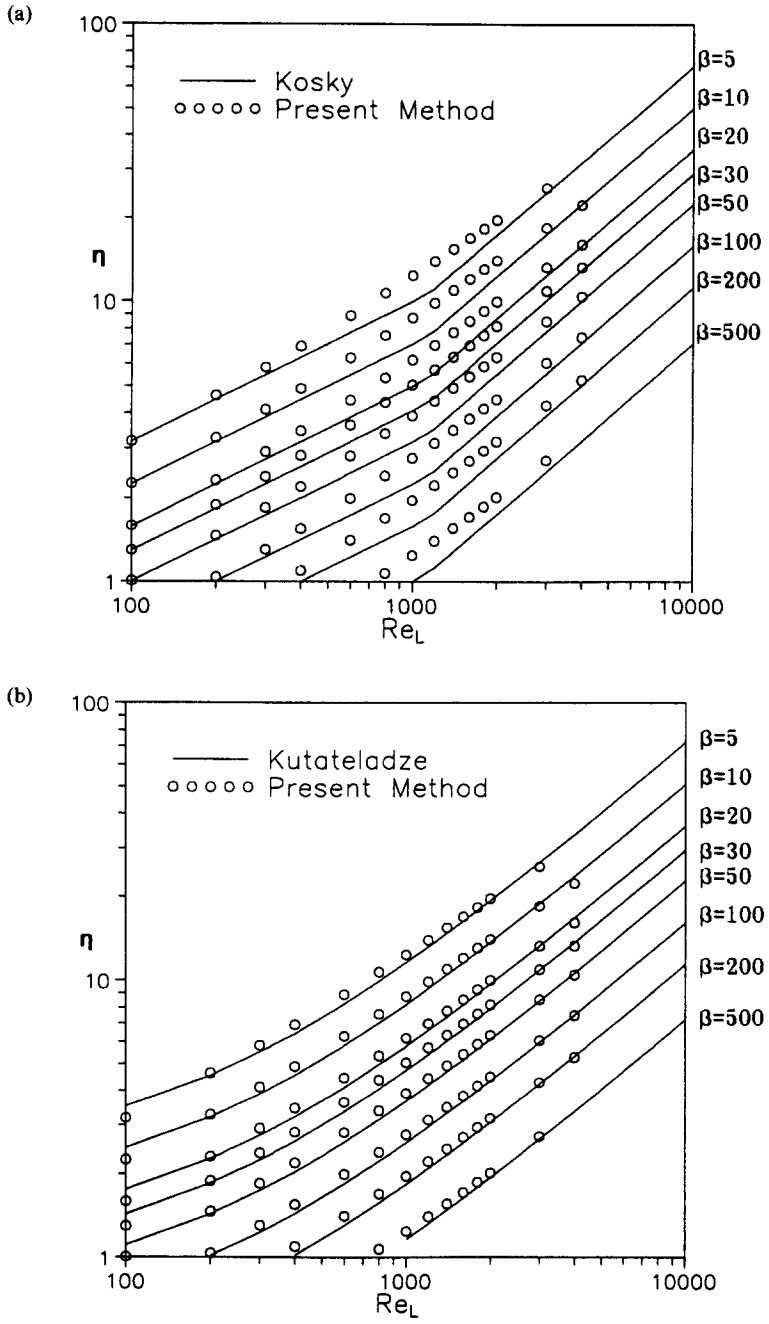

Figure 3. Comparisons of the numerical results with the formulae of (a) Kosky (1971) and (b) Kutateladze (1963).

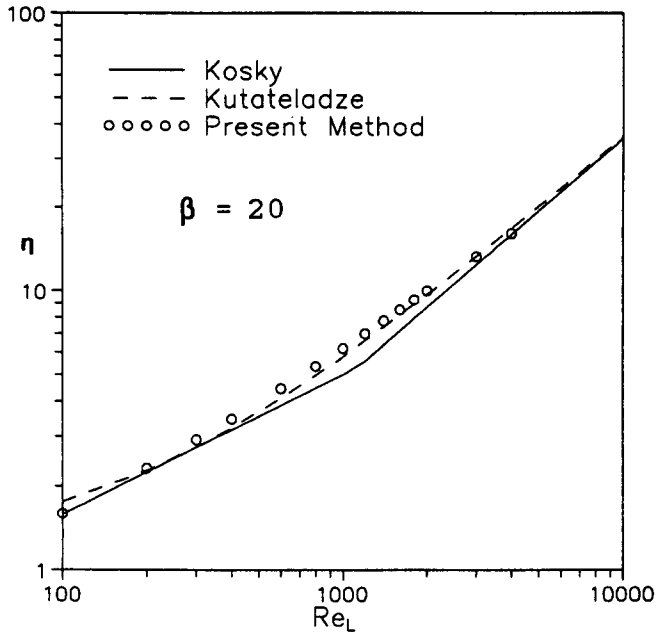

Figure 4. Comparisons of the numerical results with the formulae of Kosky (1971) and Kutateladze (1963), for $\beta = 20$.

A and B, respectively. Once the type of interfacial waves is identified, the characteristic length scale k_S of the interaction between the waves and the shear layer flow and the substrate film thickness h_S is calculated.

Cohen & Hanratty (1968) have reported, in the case of relatively thick films, that the ratio of the equivalent sand roughness to the root-mean-square (RMS) of the fluctuations in the film's time-mean height $\Delta h'$, is approximately constant, namely

$$k_S = 3\sqrt{2}\Delta h'. \qquad [18]$$

For periodic waves, $\Delta h'$ is related directly to the mean wave height H through a simple relation:

$$\Delta h' = \frac{H}{2\sqrt{2}}. \qquad [19]$$

The height H is deduced from the periodic waves model, described in appendix A. On the other hand, the solitary waves model of appendix B provides all the necessary geometric data for the calculation of $\Delta h'$, based on its definition

$$\Delta h' = \sqrt{\frac{1}{\lambda}\int_0^{\lambda} (h - \bar{h})^2 \, dl}, \qquad [20]$$

where λ is the wavelength. When the examined film flow is not in conformity with the assumptions used to derive [17]–[20], the latter must be used with reservations.

5. SOLUTION ALGORITHM

The successive steps of the solution algorithm are presented below.

Step 1

External flow data for zone I are provided, concerning the distribution of the velocity components and the pressure gradient for the gaseous phase and all the necessary information for the complete description of the dispersed phase that enters or leaves the shear layer (zone II), in

the form of the droplets' velocity vector, diameter, temperature and number density distribution. All the above data are the outcome of an inviscid two-phase code.

Step 2

The coupled two-phase shear layer/liquid film solution takes place for zones II and III. This is done by a space-marching procedure, whose main feature is that the calculation proceeds one step forward after all the necessary flow quantities in the previous location have been computed, for both the shear layer and the liquid film flows. The above calculation is performed in the following iterative manner.

Step 2.1. The "local" iterative scheme starts by assuming that all dependent variables at the current location are assigned the same values as those already calculated at the previous one.

Step 2.2. Shear layer (zone II) equations [1] and [2] are first solved, under the assumed liquid film evolution, along with the droplet transport equations.

Step 2.3. The liquid film (zone III) equations [9a] and [10] are solved in turn, making use of the calculated driving interfacial shear and the increment in the liquid flux due to droplet deposition. In this step, the film submodels, which were presented above, are used fully.

These calculations are repeated until convergence is obtained, thus providing the profiles of the flow quantities across both the shear layer and the liquid film, at the current location. This completes one forward step. Step 2 is repeated for all the computational locations along the solid wall.

Step 3

Once the shear layer characteristics are found at all the positions along the solid surface, the transpiration velocities, acting as sources of momentum in the external-inviscid flow (zone I), are calculated and introduced in the two-phase inviscid calculation (Step 1).

Steps 1–3 are repeated up to the global convergence of the viscous–inviscid interaction procedure.

6. RESULTS

6.1. *Asymptotic behaviour of liquid films on flat plates*

Validation of the liquid film velocity profile in use and of the asymptotic behaviour of the present method is attempted here. The comparisons stand for tap water film calculations along flat plates under the simultaneous influence of interfacial stresses and gravity effects. A number of experiments

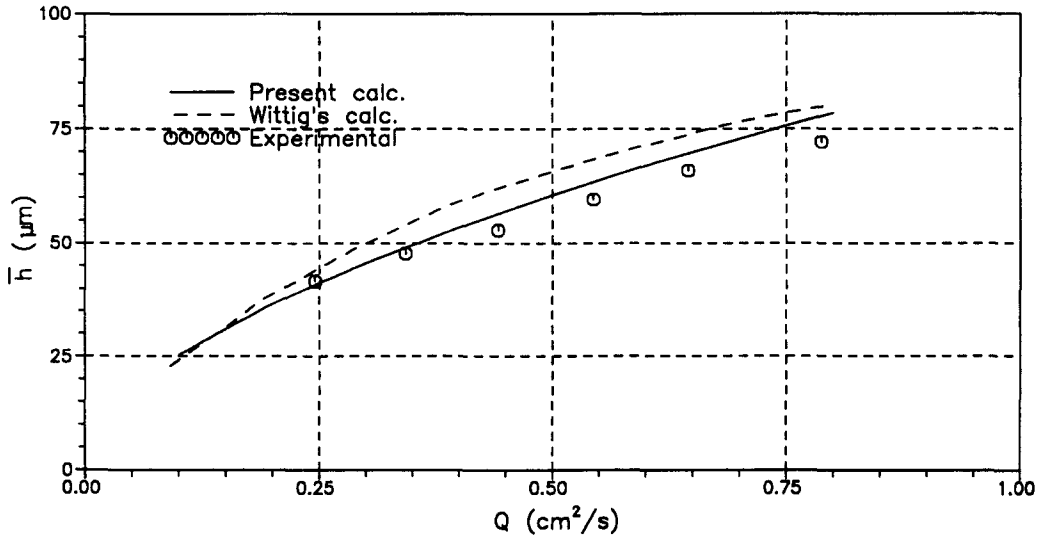

Figure 5. Time-mean film thickness for different film flow rates.

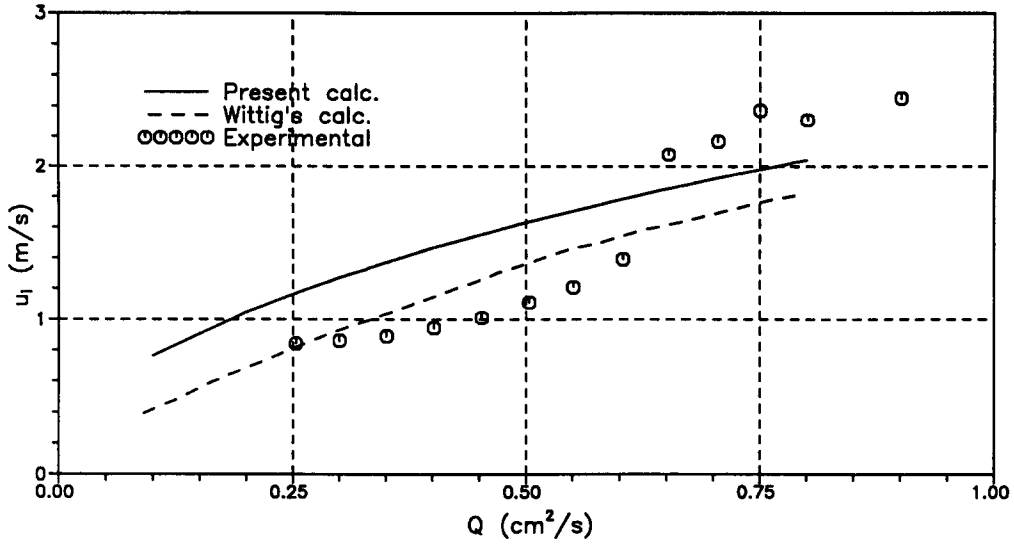

Figure 6. Interfacial velocity for different film flow rates.

were collected and analysed by Dukler (1960) and Dukler & Wicks (1963). These experiments cover different flow configurations including:

—vertical flows without interface shear ($\beta = 0$);
—vertical flows with interface shear ($\beta \neq 0$);
—and horizontal flows with interface shear ($\beta \neq 0$).

The analysis was based on a non-dimensional shear parameter β and a non-dimensional film height η, defined as

$$\beta = \frac{\left(\frac{\tau_i}{\rho_i}\right)}{g^{2/3}\nu_L^{2/3}}, \quad \eta = \bar{h}\left(\frac{g}{\nu_L^2}\right)^{1/3}. \qquad [21]$$

An additional parameter used was the film Reynolds number ($\mathrm{Re}_L = 4Q/\nu_L$) which non-dimensionalizes the volumetric flow rate Q per unit width. Here, instead of directly comparing against the numerous experimental results or the approximations proposed by Dukler, comparisons are presented against the analytical formulation of Kutateladze (1963) and Kosky (1971). These formulations showed a good agreement with the aforementioned experiments and were easy to programme.

According to Kutateladze (1963), the non-dimensional film height is deduced from a simple formula, under the assumption of logarithmic profile across the film and a two-region turbulent flow analysis. The formula was

$$\bar{h}^+(12 + 10 \ln \bar{h}^+) - 156 = \mathrm{Re}_L. \qquad [22]$$

On the other hand, Kosky (1971) succeeded in reducing Dukler's curves into a single function of one variable, taking into account both interfacial shear and gravity terms. The non-dimensional film thickness $\bar{h}^+$ is calculated through the two-region function

$$\bar{h} = \bar{h}^+(\mathrm{Re}_L) = \begin{cases} \left(\frac{\mathrm{Re}_L}{2}\right)^{1/2}, & \mathrm{Re}_L < 1000 \\ 0.0504(\mathrm{Re}_L)^{7/8}, & \mathrm{Re}_L > 1000. \end{cases} \qquad [23]$$

This resulted from the distinction between regions where a linear velocity distribution ($u^+ = y^+$) is used and others where the 1/7 th power law ($u^+ = 8.74y^{+1/7}$) is applied. The algebraic formula relating the two non-dimensional film thicknesses $\bar{h}^+$ and η is

$$\bar{h}^+ \simeq \eta(\eta \sin\theta + \beta)^{1/2}, \qquad [24]$$

where θ is the inclination angle of the plate.

Figure 3(a) interprets graphically relations [23], transformed in a parametric form similar to the one proposed by Dukler (1960) and Dukler & Wicks (1963). In the same figure, the results of the present analysis are also shown. It is worthy of mention that:

(a) The present results are all for horizontal planes.
(b) Marks correspond to the asymptotic mean film height obtained after the necessary length, with constant interfacial stress (τ_i or β) and zero pressure gradient.
(c) The calculated heights are independent of the initial film height (if, of course, the inlet height is physically acceptable and the solution covers a sufficient length, in order to reach its final asymptotic value).

Figure 3(b) compares Kutateladze's formulae with the calculated results of the present analysis. It is evident that the numerical results are satisfactorily close to the theoretical ones. Comparing figures 3(a) and (b), one can observe that the present results are closer to those of Kutateladze, rather than to Kosky's approach, for moderate Re_L. This was to be expected since Kutateladze based his analysis on a logarithmic velocity profile for the film, similar to the one used in the present method. On the other hand, for thinner films ($Re_L < 1000$), the results of the present analysis become closer to Kosky's, since both approaches are based on a linear profile ($u^+ = y^+, y^+ < 5$). To better represent this trend, the numerical results are plotted along with those of Kosky and Kutateladze in figure 4, for the value $\beta = 20$.

6.2. *Motion of a shear-driven liquid film in a turbulent gas*

Wittig *et al.* (1991) presented measurements of wavy liquid films, driven by the shear stress of turbulent air flow, along a horizontal plate. Their experimental channel had a rectangular

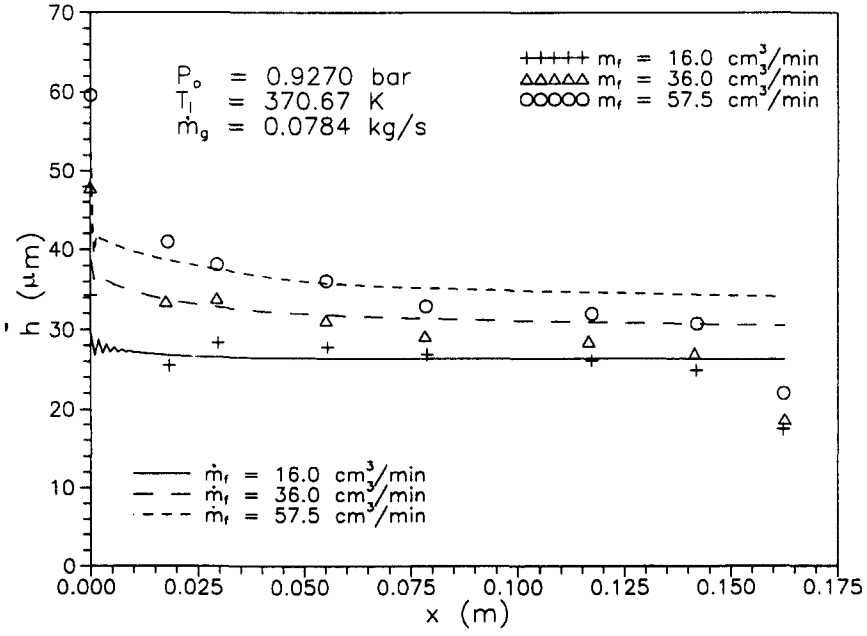

Figure 7. Time-mean film thickness evolution along the "test" blade for the (A1) set of steam conditions and for all film flow rates.

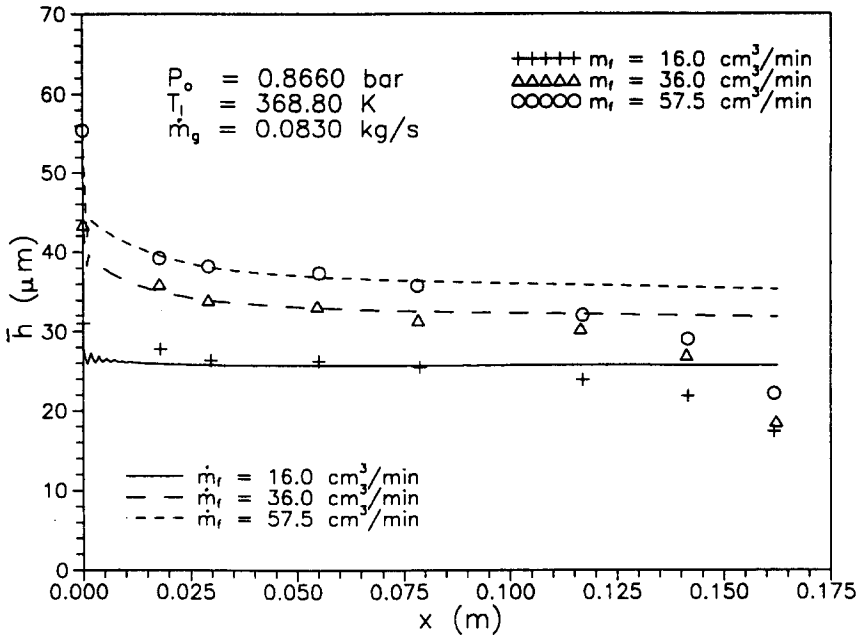

Figure 8. Time-mean film thickness evolution along the "test" blade for the (A2) set of steam conditions and for all film flow rates.

cross-section of a constant width of 60 mm; its height at the inlet was 83 mm, converging to a final one of 13 mm, which corresponds to the real test section. Along the centreline of the narrow part of the channel, a prefilming plate was placed, thus forming two equal gaps of 3.9 mm height at each side of the "test" blade. Water was supplied onto the prefilming plate through a row of holes with 0.5 mm dia and a lateral spacing of 0.8 mm. Heat transfer from the wetted wall to the film or adiabatic conditions were simulated by supplying water along one side or both sides of the prefilming plate, respectively. Their investigation was concerned with ambient pressures and temperatures up to 573 K. Measurements were taken by means of an optical apparatus and techniques based on the light absorption in the liquid. Most of them correspond to the film characteristics at a distance of 240 mm downstream of the film injection point. In the same work, the authors carried out "local" numerical calculations, based on both laminar and turbulent velocity profiles for the liquid film; their main conclusion was that the film exhibited laminar rather than turbulent characteristics. It is worth noting that for laminar films they used the linear velocity profile ($u^+ = y^+$) up to $y^+ \simeq 16$, while during the present calculations the non-dimensional time-mean height $\bar{h}^+$ was found to vary between 8 and 24.

In the present work, the developed liquid film calculation method is validated against selected test cases, presented in the aforementioned paper; for the selected cases, sufficient air and water data are provided and experimental, as well as numerical, results for the film thickness and the film surface velocity are available. With the pressure drop for the gaseous phase given in the original paper and with velocity and temperature equal to $V_G = 65$ m/s and $T_G = 573$ K, respectively, the predictions of the present method are compared with the experimental and numerical results of Wittig *et al.* (1991) in figures 5 and 6. During the present calculations, the film temperature was set equal to 90°C, for all the examined liquid film flow rates; the Re_L ranged from 31 to 245. In all the examined cases, the film surface was found to be covered by roll waves.

Figure 5 presents the two calculations along with the experimental results for the time-mean liquid film height at the aforesaid distance from the film inlet section. The present predictions compare very well with the experiment. On the other hand, figure 6 presents the interfacial film velocity, as calculated for the above cases. It can be seen that the present results, compared with those of Wittig *et al.* overestimate the interfacial velocity for all the liquid film flow rates examined herein. The interfacial velocities calculated by the present method are overestimated in the small

and minimum flow rates, compared with the experimental values, as well. On the contrary, at higher film flow rates, the interfacial velocities calculated by the present method come closer to the experimental results, compared with the calculations of Wittig *et al.* (1991). In this flow rate range, measurements do present an abrupt increase in the interfacial velocity and a question arises about the stability of the film. It is to be noted that the quantity which is compared against the measured film surface velocity is the velocity at the time-mean thickness.

6.3. Film flow over steam turbine "test" blades

Liquid film measurements along flat surfaces that are swept by steam, at velocities corresponding to flow conditions occurring in low-pressure steam turbine fixed rows, have been performed by Khoshaim & Ryley (1976). The ultimate goal of their work was to investigate the modelling of film breakdown and the formation of dry spots. The experimental procedure consisted of gradually reducing the liquid flow rate until eventually a locally zero film height was observed. In the present paper, cases corresponding to a liquid flow rate greater than the minimum wetting rate, which represents the critical film breakdown condition, are investigated. The formation of dry patches cannot be handled so far by the present method.

In the experiments, the flat blade ($7.6 \times 19 \times 1.27\,\text{cm}^3$) was positioned in the middle of a rectangular $7.6 \times 40 \times 7.6\,\text{cm}^3$ test section and was capable of being tilted to the horizontal about an axis perpendicular to the streamwise direction. In the present numerical study, the test blade coincided with the lower wall of the examined two-dimensional flow domain; the domain height was 3.16 cm, corresponding to half the height of the test section, if the blade height was also taken into account. The liquid film was introduced at the position $x = 1.25$ cm, which corresponds to the first measurement station. Nine different flow conditions were examined, for all possible combinations of the following steam and film conditions:

(A) Steam conditions

(A1) $P_t = 0.927$ bar
$T_L = 370.67$ K
$U_G = 24.8$ m/s

(A2) $P_t = 0.866$ bar
$T_L = 368.87$ K
$U_G = 30.5$ m/s

(A3) $P_t = 0.591$ bar
$T_L = 358.71$ K
$U_V = 76.2$ m/s

(B) Film volume flow rate

(B1) $Q = 3.51 \times 10^{-6}\,\text{m}^2/\text{s}$ ($\text{Re}_L \approx 10.2$ to 11.6)

(B2) $Q = 7.89 \times 10^{-6}\,\text{m}^2/\text{s}$ ($\text{Re}_L \approx 23.0$ to 26.1)

(B3) $Q = 12.61 \times 10^{-6}\,\text{m}^2/\text{s}$ ($\text{Re}_L \approx 36.7$ to 41.7)

The predictions are presented in figures 7–9 (solid or dashed lines) along with the experimental data (symbols). Each figure corresponds to a certain steam condition (A1, A2 or A3) and all the film flow rates (B1, B2 and B3). Knowledge of both the film flow rate and the inlet film thickness, renders the problem overdefined in case of a specified interfacial stress. The present calculations were based on the exact film flow rate and reasonable steam/liquid interfacial stresses; as a consequence, in figures 7–9, discrepancies exist at the inlet film height. Nevertheless, it is important to notice that a rapid thinning of the film takes place which is able to eliminate any discrepancy occurring at the inlet, within the first few calculation positions. Along the major part of the blade, a fairly constant film thickness is predicted, in accordance to the measured values. This occurs due to the fact that the steam conditions remain almost constant along the blade. The measurements reveal a sudden decrease in film thickness towards the end of the blade, probably related to a local increase in steam velocity. Such an increase in steam velocity was not imposed in the present calculation and, consequently, the local film thinning was not predicted. On the contrary, the predicted film thickness remains "uniform" to the end of the flow domain. Predictions are much closer to the experimental data for the lower film volume rates, where the film undertakes a fast transition to its asymptotic behaviour. In all the above cases, the film surface was covered with roll waves.

7. CONCLUSIONS

In the present paper a numerical method for the prediction of the coupled two-phase shear layer/liquid film development along solid surfaces is presented. The method is based on the solution of a set of conservation equations, cast in an integral form, through a space-marching technique. The description of the solution procedure, hypotheses on which the method is based and the empirical information required in order to effect closure are presented in detail. Particular attention was paid to the study of the interface phenomena, the classification of the interfacial waves and the way they are modelled. Some key elements of the developed method and the experience gained during this development are summarized below:

(1) The developed method, being very fast even on PCs, contains submodels for the various relevant physical phenomena. The modular way this method was built guarantees the easy implementation of any alternative submodel.
(2) Two-phase shear layer and liquid film calculations are fully coupled in the sense that a common space-marching algorithm is established for both the shear layer (zone II) and the liquid film (zone III). As is evident from the presented algorithm, a unique sweep of the domain is required which contains an iterative (local) shear layer/liquid film calculation at each computational location.
(3) It is to be pointed out that the present method is capable of providing the complete spatial evolution of the liquid film. The literature survey did not reveal any relevant computational method. Published models always provide information about the asymptotic behaviour of the liquid film, rather than its spatial evolution. From this point of view, the developed method is quite original.
(4) Particular physical problems, related to the liquid film calculation as a whole, could be solved if appropriate models are used, based on physical principles and reasonable assumptions. Thus, the amount of additional information required to effect closure diminishes and controllable physical models replace empirical relations and constants.
(5) Concerning the interfacial waves, two different families of waves could be handled, namely periodic and roll waves. A criterion was incorporated for the

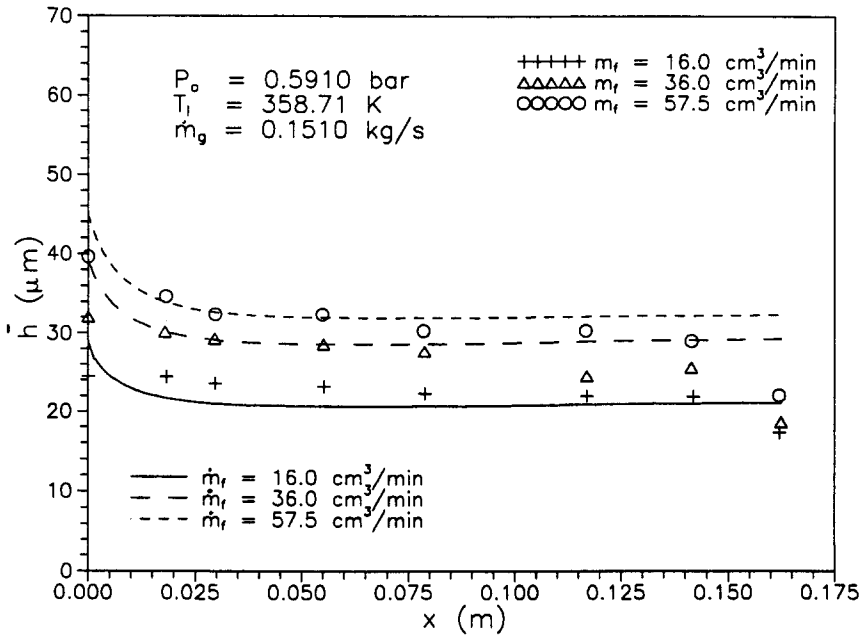

Figure 9. Time-mean film thickness evolution along the "test" blade for the (A3) set of steam conditions and for all film flow rates.

transition between the two families. Each wave category was modelled with its own model; these are models appearing in the literature and their range of applicability requires further investigation. All the built-in submodels have been carefully adapted to the "basic" flow model.

(6) Validation of the ability of the developed method was attempted in a number of representative test cases for which experimental data were available.

Acknowledgements—Part of this work was funded by the E.E.C. BRITE Project P-2156, entitled "The study of non-equilibrium two-phase flow in steam turbines". The authors wish to thank the project partners for permission to publish this paper and are grateful to Dr A. R. Laali (EDF, Chatou) for fruitful discussions.

REFERENCES

ANDREUSSI, P., ASALI, J. C. & HANRATTY, T. J. 1985 Initiation of roll waves in gas–liquid flows. *AIChE Jl* **31,** 119–126.

ANDRITSOS, N. & HANRATTY, T. J. 1987a Influence of interfacial waves in stratified gas–liquid flows. *AIChE Jl* **33,** 444–454.

ANDRITSOS, N. & HANRATTY, T. J. 1987b Interfacial instabilities for horizontal gas–liquid flows in pipelines. *Int. J. Multiphase Flow* **13,** 583–603.

BOURAS, V. 1993 Integral method for the calculation and optimization of laminar and turbulent shear layers in the presence of flow separation. Ph.D. Thesis, NTUA, Greece.

BRAUNER, N. & MARON, D. M. 1983 Modeling of wavy flow in inclined thin films. *Chem. Engng Sci.* **38,** 775–788.

BRAUNER, N., MARON, D. M. & DUKLER, A. E. 1985 Modeling of wavy flow in inclined thin films in the presence of interfacial shear. *Chem. Engng Sci.* **40,** 923–937.

CARR, J. 1981 *Applications of Centre Manifold Theory*. Springer, New York.

CHEREMISINOFF, N. P. & DAVIS, E. J. 1979 Stratified turbulent–turbulent gas–liquid flow. *AIChE Jl* **25,** 48–56.

CHU, K. I. & KUKLER, A. E. 1975 Statistical characteristics of thin, wavy films III. Structure of the large waves and their resistance to gas flow. *AIChE Jl* **21,** 583–593.

COHEN, L. & HANRATTY, T. J. 1968 Effect of waves at a gas–liquid interface on a turbulent air flow. *J. Fluid Mech.* **31,** 467–479.

COLES, D. 1955 The law of the wake in the turbulent boundary layer. Guggenheim Aero. Lab., Caltech, Pasadena, CA.

COLES, D. 1956 The law of the wall in turbulent shear flow. In *50 Jahre Grenzschicht Forschung*. Vieweg, Braunschweig.

CRAIK, A. D. 1968 Wind-generated waves in contaminated liquid films. *J. Fluid Mech.* **31,** 141–161.

CROWE, C. T. 1982 Review—numerical models for dilute gas–particle flows. *ASME Jl Fluids Engng* **104,** 297–303.

DOBRAN, F. 1983 Hydrodynamic and heat transfer analysis of two-phase annular flow with a new liquid film model of turbulence. *Int. J. Heat Mass Transfer* **26,** 1159–1171.

DUKLER, A. E. 1960 Fluid mechanics and heat transfer in vertical falling-film systems. *Chem. Engng Prog.* **56,** 1.

DUKLER, A. E. 1972 Characterization, effects and modelling of the wavy gas–liquid interface. In *Progress in Heat and Mass Transfer*, pp. 207–234. Pergamon Press, New York.

DUKLER, A. E. & WICKS, M. 1963 Gas–liquid flow in conduits. In *Modern Chemical Engineering*, Vol. 1, Chap. 8 (Edited by ACRIVOS, A.). Reinhold, New York.

HAMMITT, F. G., HWANG, J. B. & KIM, W. 1975 Liquid film measurements in the University of Michigan wet steam tunnel. ORA Report UNICH 012449-23-I.

HANRATTY, T. J. 1983 Interfacial instabilities caused by air flow. In *Waves on Fluid Interfaces* (Edited by MEYER, R. E.), pp. 221–259. Academic Press, New York.

HENSTOCK, W. H. & HANRATTY, T. J. 1976 The interfacial drag and the height of the wall layer in annular flows. *AIChE Jl* **22,** 990–1000.

HWANG, S.-H. & CHANG, H.-C. 1987 Turbulent and inertial roll waves in inclined film flows. *Phys. Fluids* **30,** 1259–1268.

JURMAN, L. A. & MCCREADY, M. J. 1989 A study of waves on thin liquid films sheared by turbulent gas flows. *Phys. Fluids* **A1,** 522–536.

JURMAN, L. A., BRUNO, K. & MCCREADY, M. J. 1989 Periodic and solitary waves on thin horizontal, gas-sheared liquid films. *Int. J. Multiphase Flow* **15,** 371–384.

KHOSHAIM, B. H. & RYLEY, D. J. 1976 Rivulet flow over steam turbine blades. In *Two-phase Transport and Reactor Safety (Proc. Two-phase Flow and Heat Transfer Symp.—Workshop, Florida, U.S.A., 18–20 Oct. 1976)*, Vol. 3 (Edited by VEZIROGLU, T. N. & KAKAC, S.), pp. 79–102. Hemisphere, Washington, DC.

KOSKY, P. G. 1971 Thin liquid films under simultaneous shear and gravity forces. *Int. J. Heat Mass Transfer* **14,** 1220–1224.

KUTATELADZE, S. S. 1963 *Fundamentals of Heat Transfer*, Chap. 15 (Edited by CHESS, R. D.). Academic Press, New York.

LOCK, R. C. & WILLIAMS, B. R. 1987 Viscous–inviscid interactions in external aerodynamics. *Prog. Aerosp. Sci.* **24,** 51–171.

MALAMATENIOS, CH. 1993 A calculation method for prediction of two-phase flows in steam-turbines. Ph.D. Thesis, NTUA, Greece.

MALAMATENIOS, CH., GIANNAKOGLOU, K. & PAPAILIOU, K. D. 1990 A calculation method for gas–droplet flows in turbomachinery components including viscous effects. In *Proc. Int. Symp. on Engineering Turbulence Modelling and Measurements, Dubrovnik, Yugoslavia, 18–20 Sept. 1990* (Edited by RODI, W. & GANIC, E. N.), pp. 917–926. Elsevier, New York.

MALAMATENIOS, CH., GIANNAKOGLOU, K. & PAPAILIOU, K. D. 1992 An integral shear layer method for the numerical prediction of steam–droplet flows. *Int. J. Multiphase Flow* **18,** 89–101.

MIYA, M., WOODMANSEE, D. E. & HANRATTY, T. J. 1971 A model for roll waves in gas–liquid flow. *Chem. Engng Sci.* **26,** 1995–1931.

MOORE, M. J. & SIEVERDING, C. 1976 *Two-phase Steam Flow in Turbines and Separators.* Hemisphere, Washington, DC.

PAPAILIOU, K. D. & BOURAS, V. 1990 Arbitrary blade section design based on viscous considerations. *von Karman Institute Lecture Series on Inverse Methods in Airfoil Design for Aeronautical and Turbomachinery Applications, VKI LS-90 PR*90-05.

PRANDTL, L. 1904 Uber flussigkeitsbewegung bei sehr kleiner Reibung. In *Proc. 3rd Int. Math. Congr.* Heidelberg, pp. 484–491.

RYLEY, D. J. & PATEL, P. D. 1973 Condensation on the surface of a low-pressure steam turbine suction blade. *Proc. Instn Mech. Engrs* **187,** 699–708.

SCHLICHTING, H. 1979 *Boundary-layer Theory*, pp. 615–626. McGraw–Hill, New York.

WITTIG, S., HIMMELSBACK, J., NOLL, B., FELD, H. J. & SAMENFINK, W. 1991 Motion and evaporation of shear-driven liquid films in turbulent gases. *J. Engng Gas Turb. Power* **114,** 395–400.

WOODMANSEE, D. E. & HANRATTY, T. J. 1969 Mechanism for the removal of droplets from a liquid surface by a parallel air flow. *Chem. Engng Sci.* **24,** 299–307.

APPENDIX A

Linear analyses, based on Orr-Sommerfeld type equations, are not able to provide any information about the amplitude of periodic waves (Craik 1968). Using boundary layer considerations, compatible with those used in the present formulation, Jurman & McCready (1989) derived a weakly non-linear wave equation, describing the evolution of the film surface elevation y with respect to the time-mean thickness $\bar{h}$, in a coordinate system moving with the wave celerity c_r. The waves were considered as individual travelling forms and the results were the celerity c_r and the wave growth rate kc_i. In a second work by Jurman *et al.* (1989), the boundaries of the qualitative behaviour of the steady solutions, separating regions where no steady solutions exist from periodic waves, were obtained using the double-zero point analysis (Carr 1981). In this appendix, the above method is extended further in order to be able to predict, apart from the speed of periodic waves and the region of their occurrence, their amplitude as well.

The non-dimensional wave equation is approximated through a system of first-order equations of the form

$$\begin{bmatrix} y_\xi \\ y_{\xi\xi} \end{bmatrix} = \begin{bmatrix} 0 & 1 \\ \mu_1 & \mu_2 \end{bmatrix} \begin{bmatrix} y \\ y_\xi \end{bmatrix} + \begin{bmatrix} 0 \\ ay^2 + byy_\xi \end{bmatrix}, \qquad [A1]$$

where the subscripts denote differentiation with respect to ξ ($\xi = x - c_r t$) and the envolved coefficients are derived directly from the work of Jurman *et al.* (1989). System [A1] possesses three fixed points which represent stationary solutions. One of them is the uniform film solution ($y = y_\xi = 0$) and the other is a shock solution ($y = -\mu_1/a$, $y_\xi = 0$).

According to Hwang & Chang (1987), the amplitudes of the periodic solutions, that bifurcate from fixed point 1 ($\mu_1 > 0$) near the double-zero singularity, are given by

$$y_{\max} = \begin{cases} 1 + |\mu_1/a|\alpha_1, & \text{if } \epsilon = 1 \\ 1 + |\mu_1/a|\alpha, & \text{if } \epsilon = -1 \end{cases} \qquad [A2]$$

and

$$y_{\min} = \begin{cases} 1 + |\mu_1/a|\alpha, & \text{if } \epsilon = 1 \\ 1 + |\mu_1/a|\alpha_0, & \text{if } \epsilon = -1, \end{cases} \qquad [A3]$$

where $\epsilon = -a/|a|$ and α and $\alpha_{1,0}$ are constants (Malamatenios 1993).

The maximum and minimum values of the periodic solutions that bifurcate from fixed point 0 ($\mu_1 < 0$) are given by

$$y_{\max} = \begin{cases} 1 + |\mu_1/a|(\beta_1 - 1), & \text{if } \epsilon = 1 \\ 1 + |\mu_1/a|(\beta - 1), & \text{if } \epsilon = -1 \end{cases} \qquad [A4]$$

and

$$y_{\min} = \begin{cases} 1 + |\mu_1/a|(\beta - 1), & \text{if } \epsilon = 1 \\ 1 + |\mu_1/a|(\beta_0 - 1), & \text{if } \epsilon = -1, \end{cases} \qquad [A5]$$

where β and $\beta_{1,0}$ are the new parametrizing constants.

The maximum and minimum wave elevations, [A2]–[A5], are non-dimensionalized using the time-mean thickness $\bar{h}$ of the liquid film. Apart from the thickness $\bar{h}$, which is known from the film solution (section 4.1), an additional input to the periodic wave model is the wavelength λ, which is empirically estimated. The knowledge of the minimum and maximum heights is used for the calculation of the wave height $H(=(y_{\max} - y_{\min})\bar{h})$.

APPENDIX B

When roll waves are identified (see section 4.3), their structure needs to be modelled, in order to provide the required information concerning film thicknesses, wave amplitude and interfacial velocity. An enriched form of the roll wave model proposed by Brauner *et al.* (1985), is adopted herein. This model is briefly presented below, with emphasis placed on the proposed modifications necessary for the compatibility of the model with the present formulation. It should be noted that the original model has been validated only for relatively thick films, i.e. for mean film heights of the order of 0.5 mm.

According to the adopted model, the roll wave is conceived as a composite of three different zones, namely the front, the back and the substrate zone, as illustrated in figure B1. Mass and momentum conservation are applied along each zone and partial solutions are matched at their common boundaries. The continuity equation, in moving coordinates, provides the first two-equations which could be selected from among the following three relations:

$$h_p(V_w - V_p) = h_b(V_w - V_b) = h_S(V_w - V_s) = \gamma, \qquad [B1]$$

where V_p, V_b and V_S are the "mean" film velocities at the corresponding locations, V_w is the wave velocity and γ is the discharge coefficient (constant in the moving coordinate system). In contrast

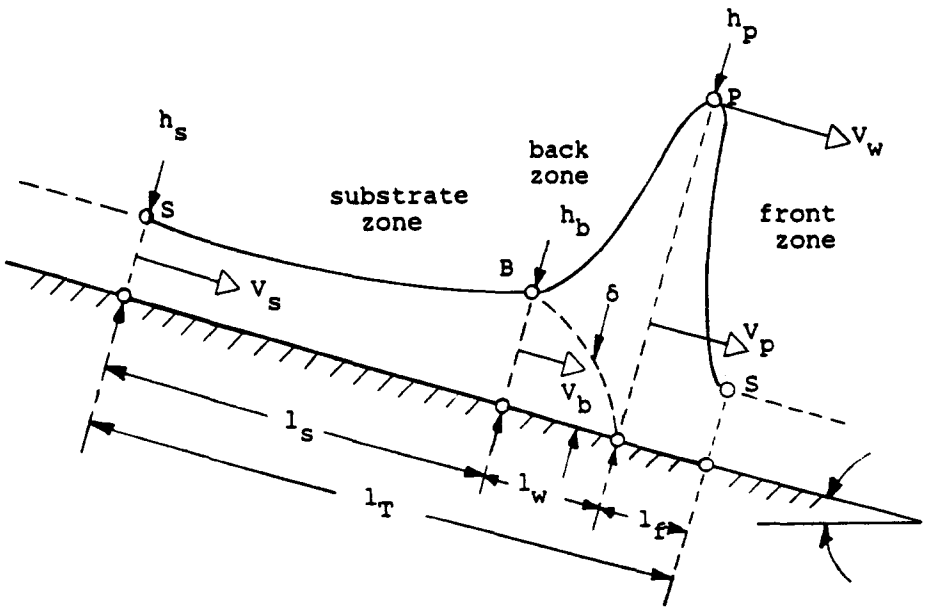

Figure B1. Schematic representation of the solitary wave model.

to the paper introducing the model, here γ is deduced from the continuity equation for the roll wave as a whole,

$$\gamma = \bar{h}V_w - Q. \qquad [B2]$$

This equation is advantageous since the mean height $\bar{h}$ consists of an input to the roll wave model, having the value calculated by [10], and Q is the known volume flux of the liquid film.

The integration of the generalized Navier–Stokes equations yields the back zone film thickness h_b, as the solution of the quadratic equation

$$h_b = -\frac{\tau_i}{\epsilon\mu_L} \pm \frac{1}{\epsilon}\sqrt{\left(\frac{\tau_i}{\mu_L}\right)^2 + 2\epsilon V_w}, \quad \epsilon = -\frac{1}{\mu_L}\left(\rho_L g \sin\theta + \frac{dP}{dx}\right). \qquad [B3]$$

A single positive root exists if $\epsilon > 0$. When $\epsilon < 0$, two positive roots appear and the smaller one is retained. Assuming parabolic velocity profiles for the film, the "mean" velocity at point S is given by

$$V_S = \frac{1}{h_S}\int_0^{h_S} u(y)\,dy = \frac{\epsilon h_S^2}{3} + \frac{\tau_i}{\mu_L}\frac{h_S}{2}. \qquad [B4]$$

Similarly, a quadratic equation is formulated for the substrate-to-back zone thickness ratio $x = h_S/h_b$:

$$\frac{\epsilon}{3}x^2 + \left[\frac{\epsilon}{3} + \frac{\tau_i}{2\mu_L h_b}\right]x + \frac{\epsilon}{3} + \frac{\tau_i}{2\mu_L h_b} - \frac{V_w}{h_b^2} = 0. \qquad [B5]$$

The momentum balance at the wave front and trail, reads

$$\rho_L[(V_w - V_S)^2 h_S - (V_w - V_p)^2 h_p] = \mu_L \epsilon\left(\frac{h_S + h_p}{2}\right)\lambda_f + (\tau_i - \tau_w)\lambda_f + \frac{\rho_L g\cos\theta}{2}(h_p^2 - h_S^2) \qquad [B6]$$

and

$$\rho_L[h_p(V_p - V_w)^2 - h_b(V_b - V_w)^2] = \mu_L \epsilon\left(\frac{h_p + h_b}{2}\right)\lambda_w + (\tau_i - \tau_w)\lambda_w - \frac{\rho_L g\cos\theta}{2}(h_p^2 - h_b^2). \qquad [B7]$$

Applying the hypothesis of the periodical distortion of the hydrodynamic boundary layer, which starts to develop from the wave front, and defining the length of the wave back as the point where the boundary layer reaches a thickness of h_b, yields

$$\lambda_w = \frac{\rho_L}{\mu_L}\frac{V_w h_b^2}{8}\left[1 - \left(\frac{2-K}{K}\right)^2\right]. \qquad [B8]$$

A detailed discusson about the shear factor K can be found in Brauner & Maron (1983). The total wavelength λ is defined as

$$\lambda = \lambda_f + \lambda_w + \lambda_S \qquad [B9]$$

and the overall material balance reads

$$\frac{\lambda Q}{V_w} = [\lambda_S h_S + \tfrac{1}{2}(h_p + h_b)\lambda_w + \tfrac{1}{2}(h_p + h_S)\lambda_f] - \frac{\lambda\gamma}{V_w}. \qquad [B10]$$

Equations [B1]–[B10] constitute a system of 11 equations which are solved to calculate all quantities related to the frontal wave region (λ_f, h_p, V_p), the wave back region (λ_w, h_b, V_b) and the wave substrate (λ_S, h_S, V_S), as well as 3 wave-related quantities (celerity V_w, wavelength λ and discharge coefficient γ). Thus, the definition of 1 of the above 12 variables is required in order to close the system of 11 equations at hand. The externally imposed quantity is the wavelength λ, since it can be empirically correlated to the mean height $\bar{h}$ of the liquid film. According to Hanratty (1983), the wavelength of roll waves formed on thin liquid films is about 25 times the time-mean film height.